Simulated structure and imaging of NTCDI on Si(1 1 1)-7 × 7 : a combined STM, NC-AFM and DFT study

OPEN ACCESS
IOP Publishing
Journal of Physics: Condensed Matter
J. Phys.: Condens. Matter **27** (2015) 054004 (8pp)
doi:10.1088/0953-8984/27/5/054004

Simulated structure and imaging of NTCDI on Si(1 1 1)-7 × 7: a combined STM, NC-AFM and DFT study

S P Jarvis[1], A M Sweetman[1], I Lekkas[1], N R Champness[2], L Kantorovich[3] and P Moriarty[1]

[1] School of Physics and Astronomy, University of Nottingham, Nottingham NG7 2RD, UK
[2] School of Chemistry, University of Nottingham, Nottingham NG7 2RD, UK
[3] Department of Physics, King's College London, The Strand, London WC2R 2LS, UK

E-mail: Samuel.Jarvis@nottingham.ac.uk

Received 22 September 2014
Accepted for publication 17 October 2014
Published 21 November 2014

Abstract

The adsorption of naphthalene tetracarboxylic diimide (NTCDI) on Si(1 1 1)-7 × 7 is investigated through a combination of scanning tunnelling microscopy (STM), noncontact atomic force microscopy (NC-AFM) and density functional theory (DFT) calculations. We show that NTCDI adopts multiple planar adsorption geometries on the Si(1 1 1)-7 × 7 surface which can be imaged with intramolecular bond resolution using NC-AFM. DFT calculations reveal adsorption is dominated by covalent bond formation between the molecular oxygen atoms and the surface silicon adatoms. The chemisorption of the molecule is found to induce subtle distortions to the molecular structure, which are observed in NC-AFM images.

Keywords: NTCDI, Si(1 1 1), STM, AFM, DFT, adsorption, structure

(Some figures may appear in colour only in the online journal)

1. Introduction

Compared to more weakly interacting substrate materials, molecular adsorption at semiconducting surfaces is a particularly interesting system of study, in part due to the potential for controlled modification of the electronic and chemical properties of surfaces [1, 2]. In the context of attachment chemistry, Si(1 1 1)-7 × 7 stands apart due to the characteristic charge transfer processes that lead to different populations of the surface dangling bonds, therefore producing sites of varying reactivity across the surface [3]. Scanning probe microscopy (SPM), with its ability to image molecules on an individual basis, has become an invaluable tool in investigating molecular adsorption with atomic precision. For instance, both scanning tunnelling microscopy (STM) and non-contact microscopy (NC-AFM) [4] have been used to to determine the exact adsorption site of a molecule using side-by-side scans of both the individual molecule and the underlying substrate [5–7].

NC-AFM is especially useful due to the impressive level of intramolecular detail obtainable using functionalised passivated tip terminations [8]. Since individual bonds were first resolved by Gross *et al* [9], NC-AFM has been used to determine molecular adsorption [7], conformation [10], bond order [11] and recently, resolve intermolecular features in molecular networks where hydrogen bonding is expected to occur [12–14]. Recently, we have also shown for the first time that intramolecular resolution can be obtained with NC-AFM on molecular species adsorbed onto reactive semiconductor surfaces [15].

In this work, we present a combination of experimental STM and NC-AFM with theoretical density functional theory (DFT) calculations investigating the adsorption of naphthalene tetracarboxylic diimide (NTCDI) on the Si(1 1 1)-7×7 surface. Although the adsorption of NTCDI has been investigated on surfaces such as Ag:Si(1 1 1)-($\sqrt{3} \times \sqrt{3}$) R30° [16, 17] and

Au(1 1 1) [18, 19], surprisingly, there appear to be no reports of NTCDI adsorption on reactive semiconductor surfaces other than our earlier report [15]. Here we extend the results described in [15] to an analysis of the STM and NC-AFM images of the multiple adsorption geometries that NTCDI molecules can adopt on the Si(1 1 1)-(7 × 7) surface. Using a combination of intramolecular resolution NC-AFM imaging and detailed DFT calculations we determine the complete molecular adsorption geometry and reveal the underlying chemisorption interaction. Finally, we simulate STM images for the identified geometries in order to compare with the experimental results.

2. Methods

2.1. Simulation details

Our investigation is performed with *ab initio* density functional theory (DFT) simulations carried out using the SIESTA code [20] using a double-zeta polarized basis set in the generalized gradient approximation with a Perdew–Burke–Ernzerhof density functional and norm-conserving pseudopotentials. Due to the relatively large size of the unit cell only a single $\mathbf{k} = 0$ point was used for sampling the Brillouin zone in our initial adsorption geometry calculations. The atomic structure was considered relaxed when forces on atoms fell below 0.01 eV Å^{-1} .

In order to model the Si(1 1 1)-7 × 7 surface, the full 7 × 7 reconstruction was simulated using a three-layer slab [21, 22]. Hydrogen atoms were used to terminate the silicon bonds on the lower side of the slab which were kept fixed along with the bottom layer of silicon, to simulate the missing bulk. This provides the minimum slab thickness required to accurately describe the dimer-adatom-stacking fault model thus producing a system of 249 atoms (shown in the side-on view of figure 2(*f*)).

Wavefunctions for the molecular orbitals were calculated using the 'denchar' utility included with the SIESTA distribution and the electronic density difference using the lev00 utility [23]. All plots of the wavefunctions and charge density were made using the XCrySDen program [24]. Simulated STM images were obtained using the Tersoff–Hamann approximation [25] and were plotted using either the WSXM software [26] (for constant current) or the 'plstm' utility (constant z) included with SIESTA.

2.2. Experimental details

Experimental data were acquired using an Omicron Nanotechnology combined LT STM/NC-AFM operating in UHV at cryogenic temperatures of either 77 K or 5 K as noted in each figure. Clean Si(1 1 1)-7 × 7 samples were prepared by standard flash annealing to 1200 °C, rapid cooling to 900 °C and then slow cooling to room temperature. A low coverage of NTCDI was prepared by depositing the molecules from a standard Knudsen cell (heated to approximately 230 °C) onto the room temperature substrate. Following deposition the sample was immediately transferred into the scan head and left to cool before imaging.

Commercial qPlus sensors supplied by Omicron with electrochemically etched tungsten wire glued to one tine of the tuning fork were introduced into the scan head without any further preparation. We typically recorded resonant frequencies of ∼25 kHz and, based on previous measurements of similar sensors [27], assume an effective stiffness of $k \sim 2000\,\mathrm{N\,m^{-1}}$. The sensors were first prepared on a clean silicon surface by standard STM techniques (pulsing and indentation) until good STM and NC-AFM resolution was achieved. Consequently, before beginning the molecular imaging experiments we expect that the apices of the tip were silicon, rather than tungsten, terminated. Similar techniques were used to recondition the tip on the surface after molecular deposition, which may facilitate the transfer of absorbed molecules onto the tip apex.

Typically we would image a region of interest in STM mode and allow any drift or piezoelectric creep to stabilise, before then switching to imaging the same region in constant height NC-AFM. During constant height imaging, oscillation amplitudes (A_0) of between 0.1 and 0.3 nm were used. In order to eliminate any possible effect from either electronic crosstalk [28] or the so-called 'Phantom Force' [29] all NC-AFM imaging was performed at 0 V (i.e. no detectable tunnel current). All data presented here is shown raw, with the exception of topographic STM images which have had the slope of the sample removed by a plane fit. During collection of NC-AFM data, an atom tracking system [30] was used to minimise drift by applying a feed-forward correction.

3. Results

3.1. STM and NC-AFM imaging of NTCDI on Si(1 1 1)-7 × 7

A ball-and-stick illustration of the NTCDI molecule considered in our study is shown in figure 1(*a*). The molecule consists of a fourteen-membered carbon backbone terminated with an imide group on each end. Similar to a previous study by Nicoara *et al* [31] of the PTCDA:Si(1 1 1)-7 × 7 system the C=O units are expected to covalently interact with the surface adatoms, thus directing the available adsorption positions of the molecule. The molecular orbitals of the free NTCDI molecule are also shown for the HOMO, LUMO, HOMO-1 and LUMO+1 in figures 1(*b*)–(*e*) respectively.

Typical STM images of the Si(1 1 1)-7 × 7 surface following submonolayer deposition of NTCDI are shown in figure 2. The larger scale image shown in figure 2(*a*) shows many of the features commonly observed following exposure to the NTCDI source. In addition to what appears to be a slight increase in the number of native adatom vacancy defects—which appear as dark missing adatoms, potentially caused by CO and water contamination during NTCDI deposition—we also observe a substantial increase in the number of bright protrusions, presumably corresponding to adsorbed NTCDI or other potential contaminants. In particular we observe several bright (dashed circles) and dark (dotted ellipses) features each with a characteristic size, appearance and location on the Si(1 1 1)-7 × 7 unit cell.

Figures 2(*b*) and (*c*) show high-resolution STM scans of the characteristic bright and dark features, respectively,

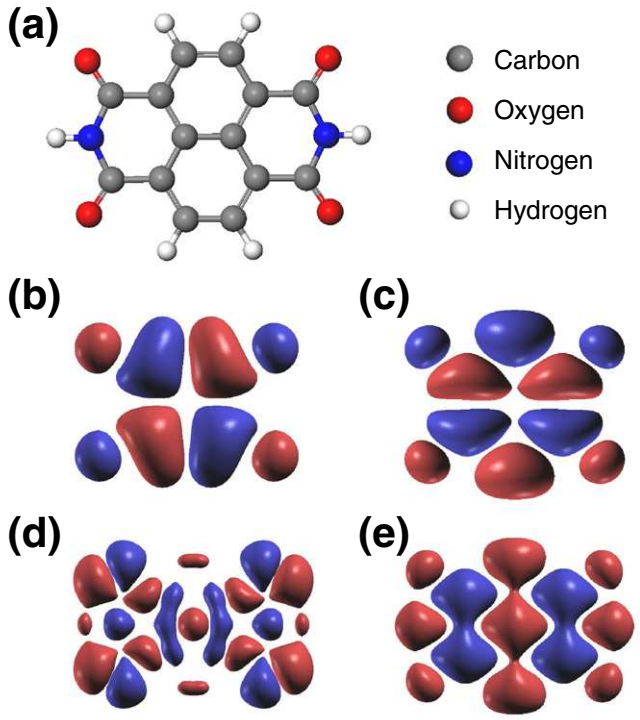

Figure 1. (*a*) Ball-and-stick structure of a NTCDI molecule. Calculated wave functions for the (*b*) HOMO, (*c*) LUMO, (*d*) HOMO-1 and (*e*) LUMO+1 for NTCDI in the gas-phase. Red/blue corresponds to positive/negative values of the wave function plotted at an isovalue of 0.01 e/a_o.

which show more detail on the lobe-like structure observed. In particular, the bright features shown in figure 2(*b*), when imaged with a positive bias, often appear as five parallel stripes aligned perpendicular to the direction separating each half of the 7 × 7 unit cell. Note that the dark features to the bottom-right of the molecule correspond to surface adatom vacancies.

The darker features show significantly less structure in STM measurements as shown in figure 2(*c*) and might easily be mistaken as clusters of adatom vacancy defects. A primary identifying characteristic of the feature is its consistent location above the silicon dimers which divide each half of the unit cell (see figure 2(*f*)), similar to the location of the bright feature in (*b*). It is therefore only due to the features' consistent size, alignment with the Si(1 1 1)-7 × 7 unit cell and subsequent NC-AFM imaging (discussed below) that we can conclusively identify the features as NTCDI molecules.

Other less commonly observed features are shown in figures 2(*d*) and (*e*). In figure 2(*d*) we show an example of an almost structureless bright feature which we assign as either an unwanted UHV contaminant, or potentially an alternative NTCDI adsorption site (see discussion on simulated STM below). Figure 2(*e*) shows a slightly more distinctive, but much rarer, structure centred over the corner hole position. As discussed below, separate NC-AFM observations suggest that this might potentially correspond to an NTCDI molecule adsorbed within the corner hole of the Si(1 1 1)-7 × 7 reconstruction, similar to previous observations with PTCDA [31].

Simultaneous or consecutive measurements of both the current and Δf (related to tip-sample force) signals using a qPlus sensor can provide detailed information on the structure of surfaces [32, 33] and molecules. Previous reports have shown that the intramolecular resolution achievable with NC-AFM can directly reveal the structure and adsorption geometry of a molecule [6, 7, 10]. In a previous investigation [15] we showed that NC-AFM can obtain intramolecular resolution on molecular species adsorbed on reactive semiconductor surfaces, specifically the same NTCDI on Si(1 1 1)-7 × 7 system considered in this study. In figure 3 we therefore acquire STM and NC-AFM images of a cluster of adsorbed NTCDI molecules appearing as a mixture of the bright and dark features shown in figures 2(*b*) and (*c*). The STM and NC-AFM images, shown in figures 3(*a*) and (*b*) respectively, were acquired immediately after one another over the same region of the surface, thus allowing us to overlay the adatom structure from the STM image onto the NC-AFM scan in (*b*) (note that a minor change in tip structure was observed during transition to NC-AFM, however the STM contrast was not significantly affected). Using this method we can clearly identify that the features in (*a*) correspond to planar adsorbed NTCDI molecules located above the connecting dimers between the two halves of the 7 × 7 unit cell, positioned perpendicular to one another.

This assignment can be confirmed by additional NC-AFM images resolving both the intramolecular features of the NTCDI molecule and the underlying adatom structure of the Si(1 1 1)-7 × 7 surface as shown in figures 4(*a*) and (*b*). Note that the alignment of the NTCDI molecule with the underlying adatoms in figure 4(*a*) can more clearly be observed in figure 5(*c*), which was taken at a larger tip-sample separation over the same molecule, with the same tip.

3.2. Density functional theory simulations

In order to gain further insight into the adsorption mechanism and geometries adopted by NTCDI we carried out *ab initio* calculations of the combined NTCDI:Si(1 1 1)-7 × 7 system using DFT as employed through the SIESTA code (see methods). Through a comparison with high-resolution NC-AFM images we determined two planar adsorption geometries matching the observations in figures 4(*a*) and (*b*) which we term Geometry 1 and 2 respectively, as shown in (*c*) and (*d*). In each case the adsorption of NTCDI on the surface is determined by the the formation of covalent bonds between the C=O units of the molecule and the Si adatoms. Due to its small size, the NTCDI molecule is able to form four Si–O bonds with the silicon adatoms near the centre of the unit cell in two perpendicular directions, thus explaining why two different appearances are observed in the experimental STM at the same surface site.

Based on the observed Si–O interaction we explored several alternative adsorption sites consisting of geometries comprising fewer bonds with the surface adatoms. As shown in figures 4(*e*)–(*h*) an additional four unique geometries can be obtained stabilised through two covalent bonds with the

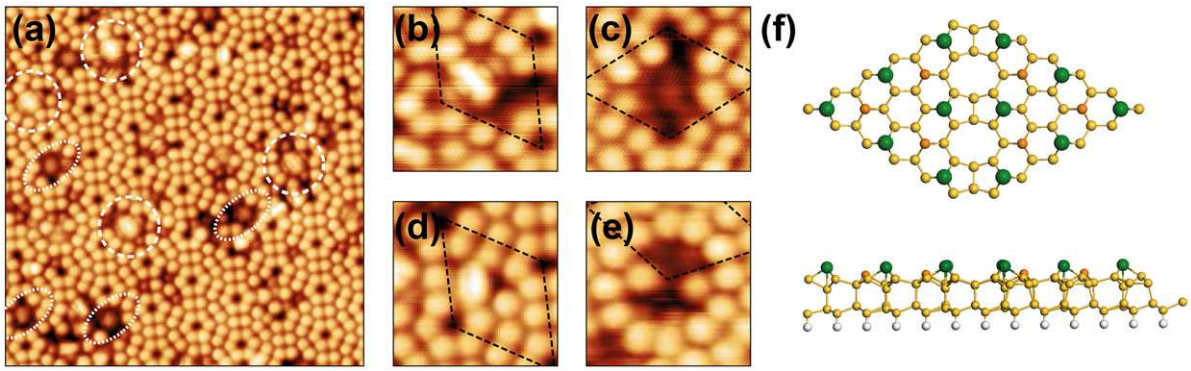

Figure 2. (*a*) STM image of the Si(1 1 1)-7 × 7 surface following a low coverage deposition of NTCDI. (*b*) Typical high-resolution image of an adsorbed NTCDI appearing as a bright feature relative to the surrounding silicon adatoms, highlighted with dashed circles in (*a*). (*c*) Adsorbed NTCDI in another configuration, appearing as a dark feature similar to a large adatom vacancy defect, highlighted with dashed ovals in (*a*). Less commonly observed features are shown in (*d*) and (*e*) potentially corresponding to alternative adsorption sites of NTCDI. Note that in (*b*)–(*e*) the 7 × 7 unit cell is indicated by a black dashed line. A schematic of the Si(1 1 1)-7 × 7 surface, representing the slab used in calculations, is shown in (*f*) with the adatoms highlighted in green, both top (above) and side (below) views are shown. Parameters: (*a*) +1.5V/70pA, scan size: 20 nm × 20 nm, $T = 77$ K, (*b*, *c*) +1.5 V/40 pA, $T = 77$ K, (*d*) +1.5 V/70 pA, $T = 77$ K, (*e*) +2 V/1.25 nA, $T = 5$ K.

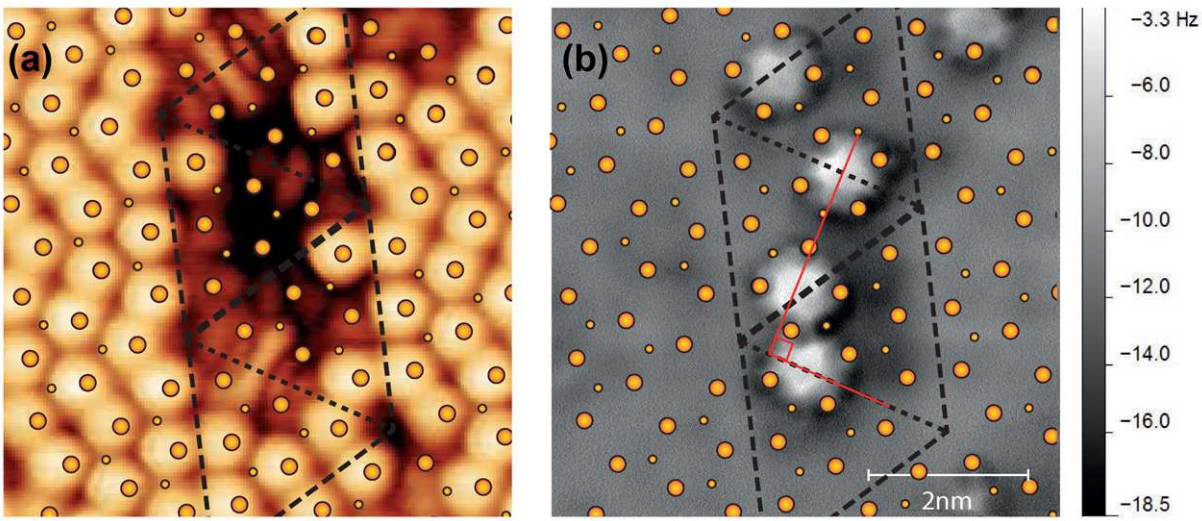

Figure 3. High-resolution (*a*) STM and (*b*) constant height NC-AFM images showing a small cluster of NTCDI molecules. The overlaid structure of the silicon surface and the surface unit cell (black dashed lines) clearly shows that the dark and bright features observed in STM correspond to two planar adsorption geometries perpendicular to one another with respect to the 7 × 7 unit cell. Parameters: (*a*) +1.5 V/40 pA, (*b*) $a_o = 280$ pm, $T = 77$ K.

surface adatoms rather than four. In this case, however, side-on views of the simulated geometry clearly show that the NTCDI no longer adopts an overall planar geometry and would likely appear asymmetric in the experimental images as shown for other molecules exhibiting strong tilting of the molecular plane [7]. As discussed below, however, some of the identified non-planar geometries might be responsible for certain features observed in STM.

A notable feature of the calculated structures for Geometry 1 and 2 is the strain-induced curvature of the NTCDI molecule caused by the molecule-surface distortions required to form the Si–O bonds. This is more clearly shown in figure 5(*a*) in a side-on DFT simulated ball-and-stick structure for Geometry 1 where the difference in height between the central carbon and peripheral nitrogen atoms is calculated to be ∼0.2 Å (∼0.35 Å for Geometry 2). As already mentioned above, this is a direct consequence of the Si–O bonds formed between the NTCDI and the surface adatoms as shown in figure 5(*b*) where the induced electron density difference (EDD) is visualised. EDD analysis shows that adsorption of NTCDI induces significant charge redistribution, primarily from the oxygen atoms of the NTCDI, in order to form a chemical bond with the surface. Whilst the separation of the central silicon adatoms (measured from the DFT-calculated structure) is ∼7.8 Å and ∼6.8 Å across the short and long axis of the Si(1 1 1)-7 × 7 unit cell respectively, the separation of the oxygen atoms in NTCDI is just ∼7.2 Å across the long axis and ∼4.6 Å across the short axis. Therefore the adatom separation outstretches that of the NTCDI by 0.6 Å and 2.2 Å in Geometry 1 and 2 respectively, forcing both the surface adatoms and the molecule to distort their structure in order to reduce the separation.

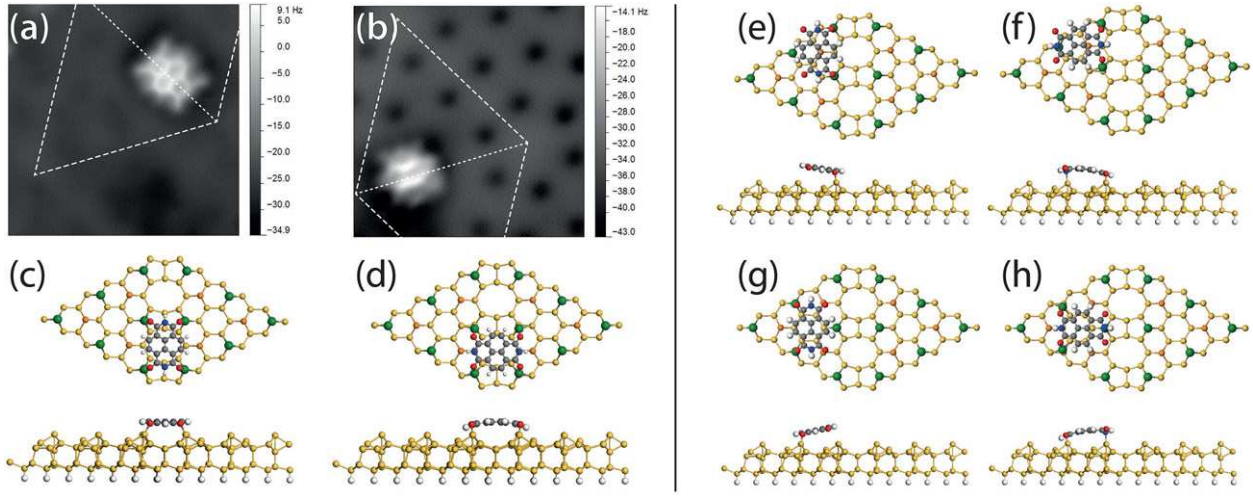

Figure 4. High-resolution NC-AFM images of each of the two primary adsorption positions, which we term Geometry 1 and 2, are shown in (*a*) and (*b*), respectively. The lowest energy DFT calculated structures for each adsorption site are shown in (*c*) and (*d*) for Geometry 1 and 2, respectively. Alternative non-planar calculated structures are shown in (*e*)–(*h*) which we term Geometry 3–6, respectively. Parameters: (*a*) $a_o = 110$ pm, scan size: 4.1 nm × 4.1 nm, (*b*) $a_o = 110$ pm, scan size: 3.27 nm × 3.27 nm, $T = 5$ K.

Distortions in the NTCDI structure are also observed with NC-AFM when imaged at larger tip-sample separations (i.e. at separations where tip-induced perturbations to the molecular structure are reduced). This is shown in figure 5(*c*)—acquired with an increased tip-sample separation of 50 pm relative to figure 4(*a*)—where the central rings of the molecule appear distinctly brighter than its periphery. This feature can be reproduced from our simulations by using the calculated total electron density (TED) as a first order approximation for the expected image. This approximation is based on the assumption that the repulsive force interaction present in the tip-molecule junction—i.e. the force responsible for intramolecular resolution—can be related to the TED of the molecule. Although this has previously been shown to provide good agreement with more detailed simulations of the complete force interaction [11] it must be noted that in certain circumstances the TED fails to accurately reproduce the observed contrast [12, 13]. Figures 5(*d*) and (*e*) show two-dimensional slices of the TED plotted at a distance 1 Å and 2 Å above the molecular plane respectively. The effect is particularly noticeable at larger separations as shown in figure 5(*e*) where the central two carbon rings appear with a significantly higher intensity compared to the outer edges of the molecule.

Neglected in our analysis thus far is the possibility of corner hole adsorption of the NTCDI molecule. Although observed infrequently, in figure 6(*a*) we show one such instance of an NTCDI molecule adsorbed in the corner hole position (acquired during the same experimental session as the results presented in [15]). As explained in detail elsewhere [34], with this particular tip termination the Si(1 1 1)-7 × 7 adatoms (and restatoms) appear as bright triangular features due to a repulsive tip-sample interaction. Importantly, however, the surface adatoms are clearly visible, allowing the simple assignment of adsorption position over the corner hole.

Due to the relatively small size of NTCDI compared to the adatom separation around the corner hole it is clear that the adsorption mechanism cannot follow that observed for the primary geometries discussed thus far, *i.e. direct bonding with surface adatoms*. The two stable adsorption geometries calculated with DFT are shown in figures 6(*b*) and (*c*). Interestingly, the only structure consistent with the observations in (*a*) calculate a geometry where the NTCDI molecule sits inside the corner hole where four Si–O bonds are formed with the second layer silicon atoms as shown in (*b*). In the alternative adsorption geometry shown in (*c*) the NTCDI molecule forms a chemical bond with only two of the surface adatoms causing it to become offset from the centre of the corner hole.

It is interesting to note that the adsorption height of the NTCDI molecule (measured as the distance in Z between the undistorted surrounding silicon adatoms and the highest point of the NTCDI molecule) reduces from ∼2.05 Å and ∼1.97 Å in the Geometry 1 and 2 configurations respectively, to ∼1.60 Å in the Corner 1 arrangement which may explain why repulsive adatom features can be observed in figure 6(*a*).

Calculated adsorption energies, relative to a summation of the isolated NTCDI and Si(1 1 1)-7 × 7 systems, are shown in table 1 for each of the geometries shown in figures 4 and 6. Geometry 1 is calculated as the most stable structure, followed by Geometry 2 which is over 0.5 eV higher in energy. The preference to adopt these configurations is primarily due to the increased number of Si–O bonds formed with the surface adatoms and reduced strain as compared to the alternative structures. The next most stable adsorption configurations are Geometry 3 and 5, which each comprise only two Si–O bonds. Interestingly, whilst Geometry 4 and 6 might be expected to have similar adsorption energies to 3 and 5, their preference is significantly reduced due to significant deformations of the molecule and surface required to allow the Si–O bonds to form (see figure 4).

The corner-hole adsorption energies are more challenging to interpret, as the structure matching most closely with the experimental observations is calculated to be the least stable,

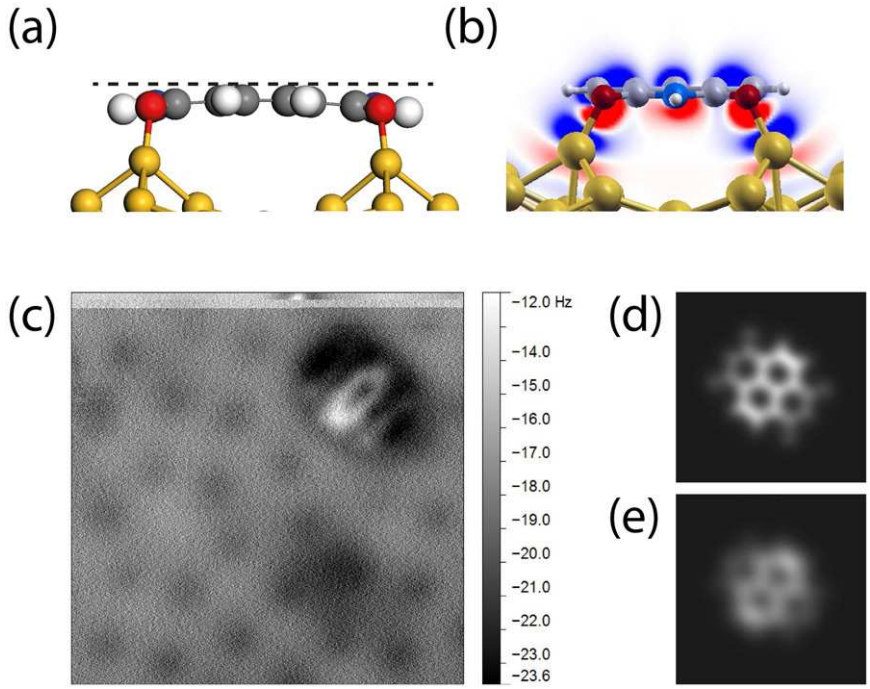

Figure 5. Distortion of the adsorbed NTCDI molecule. (*a*) Side-on ball-and-stick model of NTCDI in Geometry 1 shows curvature of the NTCDI molecule induced by surface adsorption. (*b*) Calculated electron density difference plotted as a plane cross-section intersecting the Si–O bond. Red represents density depletion and blue density excess over the range of $\pm 0.05\, e/a_o$. (*c*) NC-AFM image of the same molecule as shown in figure 4(*a*), taken at an increased tip-sample distance of 50 pm. (*d*) and (*e*) show the calculated total electron density plotted at a distance 1 Å and 2 Å above the molecular plane respectively. Parameters: (*c*) $a_o = 110$ pm, scan size: 4.1 nm × 4.1 nm, $T = 5$ K.

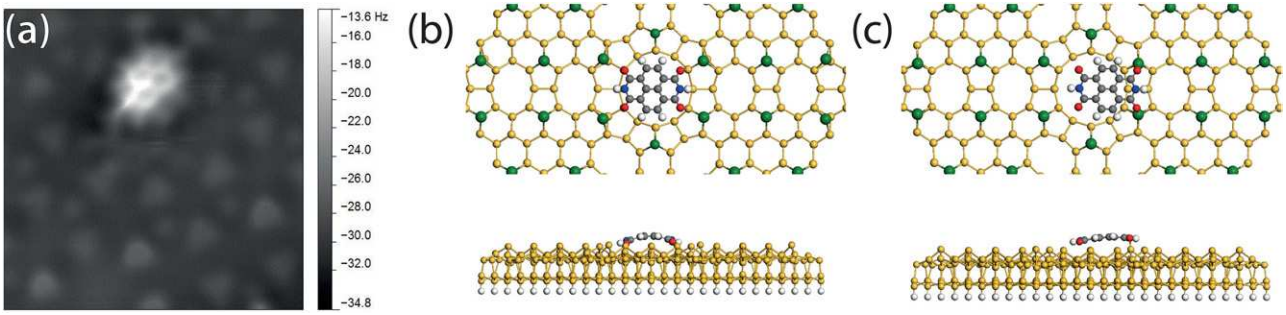

Figure 6. Corner hole adsorption of NTCDI. (*a*) NC-AFM image of a NTCDI molecule adsorbed at the corner hole site of the Si(1 1 1)-7 × 7 surface. Two calculated geometries for the corner hole position are shown in (*b*) and (*c*) termed Corner 1 and Corner 2. Parameters: (*a*) $a_o = 280$ pm, scan size: 3.5 nm × 3.5 nm, $T = 5$ K.

Table 1. Relative adsorption energies for calculated geometries of NTCDI on Si(1 1 1)-7 × 7. N refers to the total number or Si–O bonds.

	N	*Figure*	E_{ads}
Geometry 1	4	4(*c*)	−3.21
Geometry 2	4	4(*d*)	−2.67
Geometry 3	2	4(*e*)	−2.24
Geometry 5	2	4(*g*)	−2.22
Corner 2	2	6(*c*)	−1.79
Geometry 6	2	4(*h*)	−1.44
Geometry 4	2	4(*f*)	−0.80
Corner 1	4[a]	6(*b*)	+0.14

[a]Bonding involves 2nd layer silicon rather than adatoms.

less so even than the isolated systems. This is most likely explained by the absence of van der Waals forces in our simulations, which, if included, would lower the adsorption energy to a much more stable value. To explain why we only observe the Corner 1 structure, we suggest that this might potentially be explained by a complex potential energy surface. Due to its relatively small adsorption height and the recessed nature of the molecule in the Corner 1 position, it is reasonable to expect that the energy barriers required to exit this configuration might be significant enough to effectively 'trap' the molecule in this unfavourable position. We note that observing molecular adsorption in the corner hole position was a particularly rare occurrence. Although possible, in principle, a full statistical experimental analysis of each geometry would require taking many images over large surface areas with minimal changes to the STM tip.

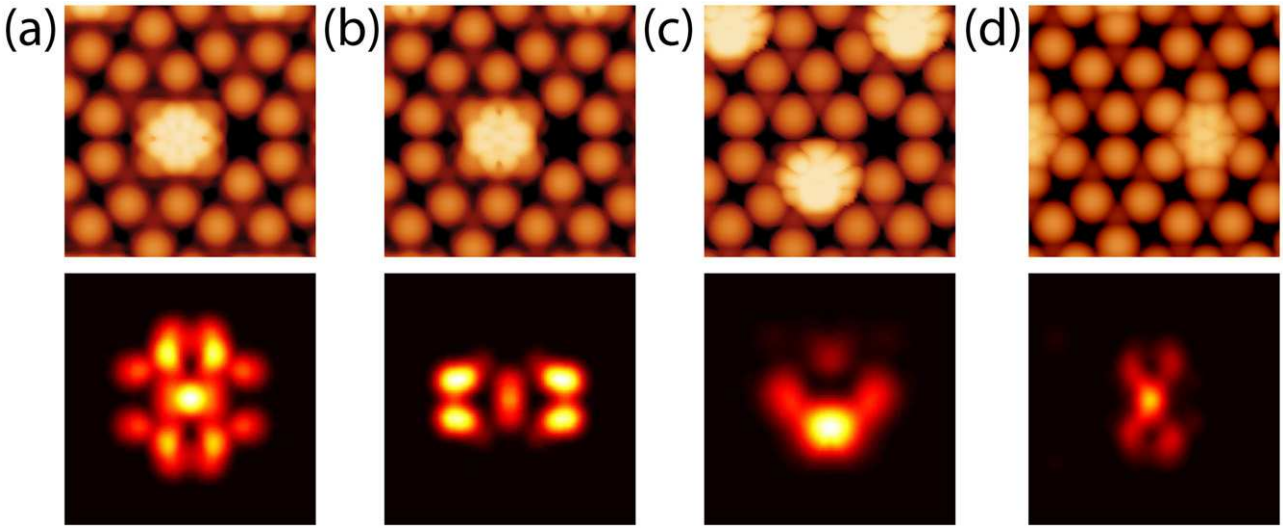

Figure 7. Simulated constant current (top) and constant z (bottom) STM images for the (*a*) Geometry 1, (*b*) Geometry 2, (*c*) Geometry 3 and (*d*) Corner 1 calculated structures. All images are calculated using a sample bias voltage of +1.5 V. Scan sizes are 3.8 nm × 3.8 nm and 1.6 nm × 1.6 nm for the constant current and constant height images respectively.

3.3. Simulated STM images

In the previous sections we have focussed on modelling the geometric structure of adsorbed NTCDI, which was compared to NC-AFM images revealing the backbone structure of the molecule. In order to examine the electronic structure we then attempted to simulate STM images using the Tersoff–Hamann approximation. Based on the calculated adsorption energies above we simulated STM images for the two lowest energy structures matching experiment, Geometry 1 and 2. In addition, we also calculated images for the Geometry 3 structure, chosen as an example metastable structure and the Corner 1 geometry, chosen due to its experimental observation in figure 6.

Figure 7 shows simulated STM images plotted as both images of constant height (bottom) and contours of constant current (top) using a sample bias of +1.5 V, chosen to match the majority of experimental observations. Considering first Geometry 1, shown in figure 7(*a*), we note that the calculated image contains many of the qualitative features observed in the experimental data. In particular, in addition to reproducing the overall bright appearance of the molecule we observe a similar shape where the central part of the molecule appears much wider (top-to-bottom in figure 7(*a*)) than each of the imide terminations. Due to the absence of a finite tip radius in our calculations, the features contributing to this overall shape can be clearly observed, particularly in the constant height image which shows five lobes of similar brightness making up the central 'band', alongside two smaller, less intense, lobes which appear at each end. Interestingly, in contrast to a previous report on PTCDA [31] we find that the simulated STM at positive biases appears dominated by the HOMO and HOMO-1 orbitals, as shown in figures 1(*b*) and (*d*), whereas images at negative biases (not shown) are dominated by the LUMO orbital, presumably due to shifts or splitting of the molecular orbitals.

Moving onto the additional calculated geometries we instead find more limited agreement. For Geometry 2 in particular (figure 7(*b*)), which is observed as a dark feature in experiments (figure 2(*c*)), we see very similar appearance to the images calculated for Geometry 1, i.e. appearing brighter than the surrounding Si(1 1 1)-7 × 7 adatoms. Similar features in the simulated STM are also observed for the Corner 1 geometry. Although in this case the molecule does appear with a reduced brightness, it is likely a consequence of the reduced molecule-surface separation and not due to significant changes to the electronic structure. Finally, for the metastable Geometry 3 we once again observe a bright appearance for the molecule, however, in this case the non-planar geometry significantly reduces the number of internal features visible in the images, similar to some of the defect-like features observed in experiment. We therefore tentatively suggest that Geometry 3 and potentially Geometries 4–6, might explain surface features such as that shown in figure 2(*d*).

We therefore conclude that whilst the simulations show some similarities to the experimental images—particularly Geometry 1 and 3—the simple Tersoff–Hamann approach is not sufficient to provide a complete model of the NTCDI:Si(1 1 1)-7 × 7 system. Indeed, Nicoara *et al* show [31], using an in-house Green's function code [35], that in order to provide better agreement with experiment more complete simulations are needed, requiring the inclusion of a model silicon tip cluster [36].

4. Conclusions

Using a combination of experimental STM, NC-AFM and theoretical DFT calculations we report a detailed analysis of the adsorption of single NTCDI molecules on the Si(1 1 1)-7×7 surface. Experimental STM images reveal multiple adsorption sites of the molecule, with two primary configurations most often observed. NC-AFM is used to image the internal structure of the adsorbed NTCDI and determine it's arrangement with respect to the underlying Si(1 1 1)-7 × 7 adatoms. A detailed analysis of the adsorption geometries

with DFT confirms two minimum energy structures matching with our experimental observations positioned above the central adatoms of the underlying Si(1 1 1)-7 × 7 unit cell. From analysis of the electronic structure we find that the interaction is dominated by the formation of Si–O bonds between the molecule and the surface adatoms, which causes buckling of the molecule, observable in our NC-AFM images. Finally, simulated STM images using the Tersoff–Hamann approximation show that the experimental STM collected at positive biases is dominated by a mix of the HOMO and HOMO-1 orbitals. However, we note that for a more complete picture, significantly more advanced STM calculations will be required.

Note added in proof. Hämäläinen *et al* (2014 *Phys. Rev. Lett.* **113** 186102) have also recently published an important paper showing, like Hapala *et al* [13], that intermolecular features can arise from tip effects. This work appeared when our paper was at proof stage.

Acknowledgments

SPJ, PM and AS thank the Engineering and Physical Sciences Research Council (EPSRC) and the Leverhulme Trust, respectively, for Grant Nos. EP/J500483/1, EP/G007837/1 and F00/114 BI. IL thanks the ACRITAS Marie Curie Initial Training Network (ITN) (PITN-GA-2012-317348) for funding. We are grateful for access to the University of Nottingham High Performance Computing Facility. NRC gratefully acknowledges receipt of a Royal Society Wolfson Merit Award.

References

[1] Buriak J M 2002 *Chem. Rev.* **102** 1271
[2] Wolkow R A 1999 *Annu. Rev. Phys. Chem.* **50** 413
[3] Tao F and Xu G Q 2004 *Accounts Chem. Res.* **37** 882
[4] Giessibl F J 2003 *Rev. Mod. Phys.* **75** 949
[5] Lagoute J, Kanisawa K and Fölsch S 2004 *Phys. Rev.* B **70** 245415
[6] Gross L, Mohn F, Moll N, Meyer G, Ebel R, Abdel-Mageed W M and Jaspars M 2010 *Nat. Chem.* **2** 821
[7] Schuler B, Liu W, Tkatchenko A, Moll N, Meyer G, Mistry A, Fox D and Gross L 2013 *Phys. Rev. Lett.* **111** 106103
[8] Mohn F, Schuler B, Gross L and Meyer G 2013 *Appl. Phys. Lett.* **102** 073109
[9] Gross L, Mohn F, Moll N, Liljeroth P and Meyer G 2009 *Science* **325** 1110
[10] Pavliček N, Fleury B, Neu M, Niedenführ J, Herranz-Lancho C, Ruben M and Repp J 2012 *Phys. Rev. Lett.* **108** 086101
[11] Gross L, Mohn F, Moll N, Schuler B, Criado A, Guitián E, Peña D, Gourdon A and Meyer G 2012 *Science* **337** 1326
[12] Sweetman A M, Jarvis S P, Sang H, Lekkas I, Rahe P, Wang Y, Wang J, Champness N R, Kantorovich L and Moriarty P 2014 *Nat. Commun.* **5** 3931
[13] Hapala P, Kichin G, Wagner C, Tautz F S, Temirov R and Jelínek P 2014 *Phys. Rev.* B **90** 085421
[14] Zhang J, Chen P, Yuan B, Ji W, Cheng Z and Qiu X 2013 *Science* **342** 611
[15] Sweetman A M, Jarvis S P, Lekkas I, Rahe P, Champness N R, Kantorovich L and Moriarty P 2014 *Phys. Rev.* B **90** 165425
[16] Perdigão L, Fontes G, Rogers B, Oxtoby N, Goretzki G, Champness N R and Beton P 2007 *Phys. Rev.* B **76** 245402
[17] Keeling D, Oxtoby N, Wilson C, Humphry M, Champness N R and Beton P H 2003 *Nano Lett.* **3** 9
[18] Ruiz-Oses M, Gonzalez-Lakunza N, Silanes Iand Gourdon A, Arnau A and Ortega J 2006 *J. Phys. Chem.* B **110** 25573
[19] Seydou M, Teyssandier J, Battaglini N, Kenfack G T, Lang P, Tielens F, Maurel F and Diawara B 2014 *RSC Adv.* **4** 25698
[20] Soler J M, Artacho E, Gale J D, Garcia A, Junquera J, Ordejon P and Sanchez-Portal D 2002 *J. Phys.: Condens. Matter* **14** 2745
[21] Rurali R, Cuadrado R and Cerdá J I 2010 *Phys. Rev.* B **81** 075419
[22] Chiutu C, Sweetman A M, Lakin A J, Stannard A, Jarvis S, Kantorovich L, Dunn J L and Moriarty P 2012 *Phys. Rev. Lett.* **108** 268302
[23] Kantorovich L N unpublished
[24] Kokalj A 2003 *Comput. Mater. Sci.* **28** 155
[25] Tersoff J and Hamann D R 1983 *Phys. Rev. Lett.* **50** 1998
[26] Horcas I, Fernández R, Gómez-Rodríguez J M, Colchero J, Gómez-Herrero J and Baro a M 2007 *Rev. Sci. Instrum.* **78** 013705
[27] Sweetman A, Jarvis S, Danza R, Bamidele J, Gangopadhyay S, Shaw G A, Kantorovich L and Moriarty P 2011 *Phys. Rev. Lett.* **106** 136101
[28] Majzik Z, Setvín M, Bettac A, Feltz A, Cháb V and Jelínek P 2012 *Beilstein J. Nanotechnol.* **3** 249
[29] Weymouth A, Wutscher T, Welker J, Hofmann T and Giessibl F 2011 *Phys. Rev. Lett.* **106** 226801
[30] Rahe P, Schütte J, Schniederberend W, Reichling M, Abe M, Sugimoto Y and Kühnle A 2011 *Rev. Sci. Instrum.* **82** 063704
[31] Nicoara N, Paz O, Méndez J, Baró A M, Soler J M and Gómez-Rodríguez J M 2010 *Phys. Rev.* B **82** 075402
[32] Sweetman A, Stannard A, Sugimoto Y, Abe M, Morita S and Moriarty P 2013 *Phys. Rev.* B **87** 075310
[33] Sweetman A, Danza R, Gangopadhyay S and Moriarty P 2012 *J. Phys.: Condens. Matter* **24** 084009
[34] Sweetman A, Rahe P and Moriarty P 2014 *Nano Lett.* **14** 2265
[35] Paz O and Soler J M 2006 *Phys. Status Solidi* B **243** 1080
[36] Paz O, Brihuega I, Gómez-Rodríguez J and Soler J 2005 *Phys. Rev. Lett.* **94** 056103